Climate Dynamics (1999) 15:561–568

J. Egger

POPs and MOPs

Received: 29 July 1998 / Accepted: 10 February 1999

Abstract Principal oscillation pattern (POP) analysis fits a first order multivariate autoregressive model to a reduced subset of the variables of a complex system. It has been shown in the past that important modes of complex systems can be detected through the POP technique. In this note two problems with this method will be addressed. Firstly, the POP analysis may face difficulties if the reduced system is of higher order in time than first. An example from linear equatorial wave dynamics is given to illustrate this point. Autoregressive models of higher order (MOP-models) are shown to provide a partial solution in such situations but are not fully satisfactory either. Nonlinearity may cause problems as well. A nonlinear low-order model is used to discuss this point. Both the POP and the MOP scheme are applied without data reduction. The MOP approach is superior to the POP technique in that it detects oscillating patterns which elude the POP analysis. The results suggest that the MOP analysis may be a valuable extension of the POP approach.

1 Introduction

Principal oscillation patterns (POPs) as introduced by Hasselmann (1988) and von Storch et al. (1988) proved useful in analyzing the space-time structure of complex systems. Although a succinct description of this technique and its application is given in von Storch et al. (1995), a brief outline of the method is provided here to set the scene. The basic idea is to construct a reduced linear model of a complex system like a climate model by fitting a first order multivariate autoregressive model to a selected subset $\mathbf{x}$ of variables of the system.

J. Egger
Meteorologisches Institut, Universität München, Theresienstr. 37, 80333 München, Germany

The model is

$$\mathbf{X}_{n+1} = \mathbf{P}\mathbf{X}_n + \mathbf{f} \tag{1}$$

where n is a time index ($t = nDt$; Dt time step) and $\mathbf{f}$ is a stochastic forcing. The matrix $\mathbf{P}$ is estimated from the data $\mathbf{x}$ (t) of the system via

$$\mathbf{P} = \hat{\Sigma}_1 \hat{\Sigma}_0^{-1} \tag{2}$$

where

$$\hat{\Sigma}_1 = \frac{1}{N} \sum_n (\mathbf{x}_{n+1} - \bar{\mathbf{x}})(\mathbf{x}_n - \bar{\mathbf{x}})^{\mathrm{T}},$$

$$\hat{\Sigma}_0 = \frac{1}{N} \sum_n (\mathbf{x}_n - \bar{\mathbf{x}})(\mathbf{x}_n - \bar{\mathbf{x}})^{\mathrm{T}} \tag{3}$$

(von Storch et al. 1995; von Storch and Zwiers 1999). In Eq. (3) N is the number of available data points in time and the bar denotes the time average. Note that data reduction, if any, is performed before the POP-analysis is carried out. The eigenvectors of the matrix $\mathbf{P}$ are the POPs with related eigenvalues $v_i = \gamma_i \exp(i\omega_i)(|\gamma_i| \leq 1$; γ_i, ω_i real). The v_i follow from Eq. (1) with $f = 0$ by assuming $X_{n+1} = v_i X_n$. It is hoped that these eigenvectors resemble typical patterns of the analyzed system. For example, Schnur et al. (1993) were able to establish a close similarity of POPs derived from atmospheric geopotential fields and eigensolutions of the related baroclinic instability problem (see von Storch et al. 1995 for further references).

On the other hand, von Storch and Zwiers (1999) caution that 'the POP method is not useful in all applications'. They argue, that the method will fail if applied to strongly nonlinear systems where linear model equations like Eq. (1) are inappropriate. Moreover, Bürger (1993) pointed out that POP-analysis cannot handle standing oscillations. He proposed an elegant extension of the POP analysis to resolve this issue. There is another problem that has received little attention so far. The POP-ansatz assumes that the system to be analyzed is described by prognostic

equations of the first order. For example, the equations governing atmospheric motion are of first order in time. However, there is no reason why the prognostic equations for a reduced system should be of first order as well. If their order is higher than one, the POP-analysis is faced with an awkward choice between frequencies. It is likely that this will lead to difficulties. An example will be given to illustrate this point (Sect. 2). This problem may be resolved by turning to autoregressive models of higher order with corresponding main oscillation patterns (MOPs).

The MOP-model

$$\mathbf{X}_{n+J} = \sum_{m=0}^{J-1} \mathbf{P}_m \mathbf{X}_{n+m} + \mathbf{f} \tag{4}$$

of order J is a straightforward extension of Eq. (1). The matrices P_m are obtained from

$$\hat{\Sigma}_{J-j} = \sum_{m=0}^{J-1} \mathbf{P}_m \hat{\Sigma}_{m+J-j} \tag{5}$$

($j = 1, \ldots J$) where $\hat{\Sigma}_{-k}$ is the transposed form of $\hat{\Sigma}_k$. The "eigenvalues" λ_i of the MOP-model result from Eq. (4) with $f = 0$ after assuming $X_{n+1} = \lambda X_n$ so that

$$\lambda^J X_n = \sum_{m=0}^{J-1} \lambda^m \mathbf{P}_m \mathbf{X}_n. \tag{6}$$

This homogeneous system of linear equations can be solved only if the determinant vanishes. This condition yields a polynominal of order $J * M$ (M number of variables constituting the vector $\mathbf{X}$). Although standard routines are available to solve polynomials it may be seen as a drawback of the MOP-approach that standard eigenvalue evaluation routines appear not to be sufficient. However, the MOP-models proposed here may be also seen as POP-models. Assume a MOP-model of second order. In that case one has just to extend the phase space for the data vector $\mathbf{x}_n$ such that it contains both the vector $\mathbf{x}_n$ and the difference

$$\mathbf{u}_n = \mathbf{x}_{n+1} - \mathbf{x}_n. \tag{7}$$

With this simple trick the MOP-model

$$\mathbf{X}_{n+2} = \mathbf{P}_1 \mathbf{X}_{n+1} + \mathbf{P}_2 \mathbf{X}_n \tag{8}$$

can be converted into the POP-model

$$\mathbf{X}_{n+1} = \mathbf{X}_n + \mathbf{U}_n,$$

$$\mathbf{U}_{n+1} = (\mathbf{P}_1 - \mathrm{I})(\mathbf{X}_n + \mathbf{U}_n) + \mathbf{P}_o \mathbf{X}_n. \tag{9}$$

This means in practice that the fitting of a MOP-model can be based on the same code as that of the POP-analysis. Given that root λ_i of the polynomial the related "eigenvector" $\mathbf{X}_i$ has to satisfy Eq. (6) with $\mathbf{X}_n$ replaced by $\mathbf{X}_i$ and λ by λ_i. This eigenvector is called the "main oscillation pattern" (MOP).

There is an obvious similarity of the MOP-model of second order to the complex POP-model as introduced by Bürger (1993). Both models rely on information about tendencies. A Hilbert transform is used to provide this information in complex POP analysis while the tendencies enter directly via Eq. (7) in the MOP-analysis. However, this similarity disappears if the order J of the MOP-model is larger than 2.

The fitting of autoregressive models to data is, of course, not new nor is the attempt to compare the performance of autoregressive models of different order (e.g. Box and Jenkins 1976; Wilks 1995). However, the example chosen in Sec. 2 is such that exact solutions are available. This allows assessment of performance of the POP and MOP models with some accuracy.

Although von Storch and Zwiers (1999) refer to nonlinearity, an investigation of the effects of nonlinearity on POPs and MOPs appears not to have been considered so far. A simple low-order model will be used to shed light on related problems (Sect. 3).

2 Data reduction

Data reduction is typically carried out in POP-analysis by projecting the original data onto eigenstructures such as EOFs and by discarding variables. As an example, linear shallow water flow on the equatorial β-plane is chosen to demonstrate related problems. The system is described by

$$\frac{\partial u}{\partial t} - \beta y v = -g' \frac{\partial \eta}{\partial \mathrm{x}} - du + w_1 \tag{10}$$

$$\frac{\partial v}{\partial t} + \beta y u = -g' \frac{\partial \eta}{\partial y} - dv + w_2 \tag{11}$$

$$\frac{\partial \eta}{\partial t} + \frac{\partial}{\partial \mathrm{x}}(Hu) + \frac{\partial}{\partial \mathrm{y}}(Hv) = -d\eta + w_3, \tag{12}$$

where (equator: $y = 0$; u zonal, v meridional perturbation flow velocity; η height perturbation; H equivalent height; g' reduced gravity; $\beta = 2\Omega/a$; $\Omega = 2\pi\mathrm{day}^{-1}$; a Earth's radius; d damping; w_i white noise forcing; see Gill 1982 for further details). Data reduction is performed by selecting a zonal wave number k and by projecting all fields on parabolic cylinder functions. For the sake of simplicity just one flow mode is selected and new complex variables $\hat{v}$, $\hat{q}$, $\hat{r}$ are introduced with:

$$v = \hat{v}(t) 2y^* \exp(-y^{*2}/2 + ikx), \tag{13}$$

$$u = \frac{1}{2}(\hat{q}(t)(4y^{*2} - 2) - \hat{r}(t)) \exp(-y^{*2}/2 + ikx), \tag{14}$$

$$\eta = \frac{c}{2g}(\hat{q}(t)(4y^{*2} - 2) + \hat{r}(t)) \exp(-y^{*2}/2 + ikx), \tag{15}$$

where $c = (g'H)^{1/2}$ is the phase speed of pure gravity waves and $y^* = y(\beta/c)^{1/2}$. It is understood in Eqs. (13)–(15) that only the real part of the right hand side is to be taken into account. The prognostic equations for $\hat{v}$, $\hat{q}$, $\hat{r}$ are (e.g. Gill 1982)

$$\frac{\partial \hat{v}}{\partial t} + d\hat{v} + 2s\hat{q} - \frac{1}{2} s\hat{r} = w'_1, \tag{16}$$

$$\frac{\partial \hat{q}}{\partial t} + ikc\hat{q} + d\hat{q} - s\hat{v} = w'_2, \tag{17}$$

$$\frac{\partial \hat{r}}{\partial t} - ikc\hat{r} + d\hat{r} + 2s\hat{v} = w'_3, \tag{18}$$

where $s = (\beta c)^{1/2}$ and where the white noise forcing w_i' differs, of course, from that in Eqs. (10)–(12). The basic eigenfrequencies of Eqs. (16)–(18) are

$$\mu_i = -i\omega_i - d \tag{19}$$

($i = 1, 2, 3$) where the real frequencies ω_i are roots of the polynomial

$$\omega^3 - (k^2c^2 + 3\beta c)\omega - \beta k c^2 = 0. \tag{20}$$

Two of the roots represent gravity waves, one root is linked to Rossby waves (e.g. Gill 1982). Elimination of $\hat{r}$, $\hat{q}$ in Eqs. (16)–(18) yields an equation of third order in time for $\hat{v}$.

Up to this pont, data compression did not involve any loss of accuracy. Thus, data provided by an integration of Eqs. (16)–(18) are of the same quality as those obtained from (10)–(12), except that now just one flow mode is involved. It is now assumed that the POP-analyst looks at the meridional wind data only. There may not be access to zonal wind and height data or there may be reasons of matrix estimation accuracy which lead to the choice of the reduced data set. For example, Schnur et al. (1993) selected the geopotential as the variable to be analyzed. They simply discarded the information contained in the wind observations. When von Storch and Xu (1990) analyzed the 200-hPa velocity potential along the equator, they excluded information on geopotential and vorticity.

The autocovariance $\langle \hat{v}\hat{v}^*(\tau)\rangle$ with lag τ is needed in order to construct the POP-model. The related calculation is cumbersome but straightforward (e.g. Honerkamp 1989). Equations (16)–(18) have to be solved and the fact that the forcing is white used to arrive at the result

$$\langle \hat{v}\hat{v}^*(\tau)\rangle = \sum_{i=1}^{3} \exp(\mu_i \tau) b_i \tag{21}$$

where the coefficients b_i depend on the parameters of the model and on the intensity of the forcing. The autocorrelation is shown in Fig. 1 for small (solid) and strong damping (dashed). The forcing intensity is the same for all three variables. The parameters are chosen such that the periods of the gravity waves are 1.7 and 1.9 days respectively, while that of the Rossby wave is 16 days. Of course, the autocorrelation is dominated by the gravity modes. The impact of friction is seen clearly: the autocorrelation decays rapidly for $d = \text{day}^{-1}$.

Given the autocorrelation Eq. (21), a POP-model can be designed according to Eq. (1). The model equations are

$$X_{n+1} = P_{11}X_n + P_{12}Y_n$$

$$Y_{n+1} = P_{21}X_n + P_{22}Y_n \tag{22}$$

where $X \sim Re(\hat{v})$, $Y \sim Im(\hat{v})$ and where the lag τ in Eq. (21) equals the time step Dt of the POP-model. The covariance matrix is immediately available from Eq. (21). The POP-model can be constructed for any choice of $Dt = \tau$, but given Fig. 1 one would choose $Dt \leq 1$ day. Note that there are no sampling problems because Eq. (21) is exact. It is not obvious a priori that the POP-model will fail in this case. Figure 1 suggests that the process to be analyzed is a damped oscillation with a clearly dominant frequency.

Results are displayed in Fig. 2 where the period M_p of the POP model is shown as a function of the length Dt of the time step. The POP-model gives a period $M_p \sim 4$ days for time steps up to one day and if just $\hat{v}$ is forced stochastically ($w_2' = w_3' = 0$; solid). This period decreases sligthly with increasing Dt. For $Dt > 1$ day, the period increases rapidly. Such an increase occurs if P_{12} approaches zero with increasing Dt. In particular, $M_p = \infty$ for $P_{12} = 0$. This zero crossing occurs earlier if all modes are forced with the same intensity (dashed). In that case $M_p \sim \infty$ for $Dt \sim 0.6$ days and the period M_p is closer to that of the Rossby wave for small Dt.

It is no surprise that the POP-model cannot cope with this situation. The POP-model has to choose between three different frequencies but there is no criterion concerning which one to choose. It is demonstrated in Appendix 1 that a similar situation arises even if there are just two frequencies.

An obvious way out of this problem is to construct a POP-model based on data from all three variables $\hat{q}$, $\hat{r}$, $\hat{v}$. If these data are unavailable, a MOP-model of third order may solve at least part of the problem. Three frequencies are available in that case and it is hoped that both the gravity wave frequencies and that of the Rossby wave will be found through a MOP-analysis.

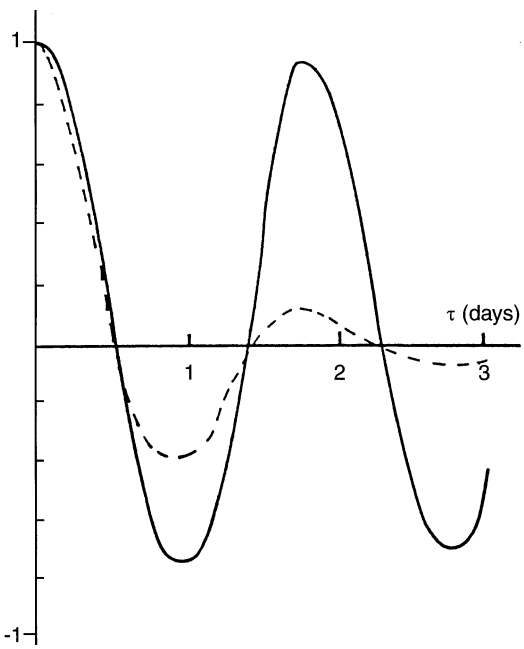

Fig. 1 Autocorrelation of the real part $Re(\hat{v})$ of the meridional flow mode coefficient $\hat{v}$ according to Eq. (21) as a function of lag τ (days). All variables forced with the same intensity. *Solid line*: damping constant $d = 1/(100$ days); *dashed*; $d =$ (day)$^{-1}$; $k = 5/a$ m^{-1}; $c = 20$ m s^{-1}

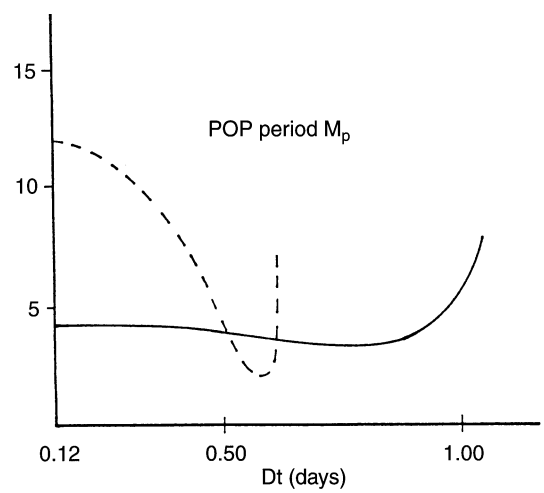

Fig. 2 Period M_p of the POP-model Eq. (22) in days adapted to the data in Eq. (21) provided by the equatorial shallow water model. *Solid line*: only $\hat{v}$ forced; *dashed*: all variables forced. $k = 5/a$ m^{-1}, $d = 10^{-6}$ s^{-1}; $c = 20$ m s^{-1}

Such a model has been constructed. The equations of the model are

$$X_{n+3} = Q_{11}X_{n+2} + Q_{12}Y_{n+2} + R_{11}X_{n+1} + R_{12}Y_{n+1} + S_{11}X_n + S_{12}Y_n$$
$$Y_{n+3} = Q_{21}X_{n+2} + Q_{22}Y_{n+2} + R_{21}X_{n+1} + R_{22}Y_{n+1} + S_{21}X_n + S_{22}Y_n \quad (23)$$

The matrices $\mathbf{Q}\sim\mathbf{P}_2$, $\mathbf{R}\sim\mathbf{P}_1$, $\mathbf{S}\sim\mathbf{P}_o$ are introduced in Eq. (23) in order to have no more than two indices. The coefficients are evaluated on the basis of Eqs (21) and (5). The submatrices of the MOP-model are antisymmetric, of course, with $\mathbf{Q}_{11} = \mathbf{Q}_{22}$, $\mathbf{Q}_{12} = -\mathbf{Q}_{21}$ etc.

As outlined already, the "eigenvalues" λ_i of Eq. (23) are obtained by assuming

$$X_{n+1} = \lambda X_n$$
$$Y_{n+1} = \lambda Y_n \quad (24)$$

and imposing the condition

$$\begin{vmatrix} -\lambda^3 + Q_{11}\lambda^2 + R_{11}\lambda + S_{11} & Q_{12}\lambda^2 + R_{12}\lambda + S_{12} \\ Q_{21}\lambda^2 + R_{21}\lambda + S_{21} & -\lambda^3 + Q_{22}\lambda^2 + R_{22}\lambda + S_{22} \end{vmatrix} = 0. \quad (25)$$

The resulting polynomial is of sixth order.

The three periods M_m of the MOP-model are displayed in Fig. 3 as a function of the damping rate d. The MOP-model of third order is excellent if the damping rate d is small. In that case all three frequencies of the basic model Eqs (16)–(18) emerge. However, the MOP-analysis fails to capture the Rossby frequency as soon as the impact of the damping is felt. It can be seen that the representation of the Rossby frequency is unsatisfactory even for quite small values of d. On the other hand, both gravity wave frequencies are captured quite well for all damping rates. The results displayed in Fig. 3 have been obtained for a time step $Dt = 5$ h. The quality of the results deteriorates quickly if $Dt > 15$ h. Similar features have been found for the POP-model (Fig. 2).

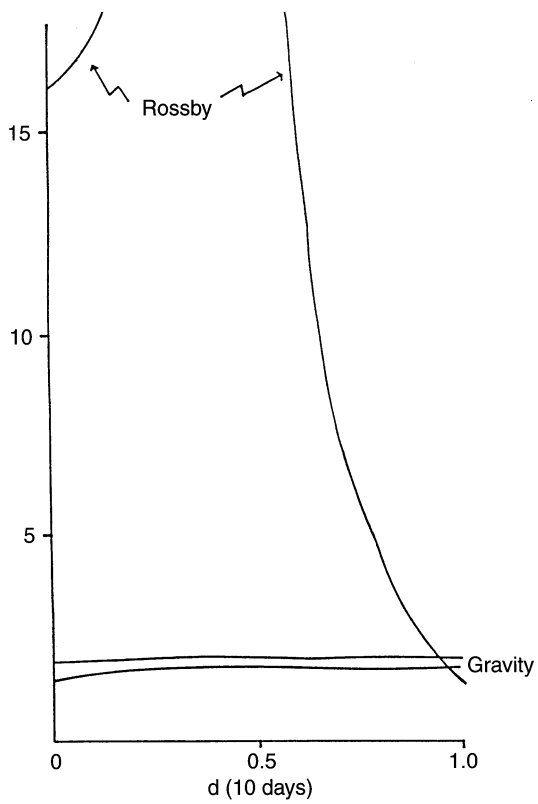

Fig. 3 Periods M_M [days] of the MOP model Eq. (23) adapted to the data Eq. (21) of the shallow water model as a function of damping d (10 days)$^{-1}$; $k = 5/a$ m^{-1}; $c = 20$ ms^{-1}; $Dt = 5$ h

The POPs are not interesting in this case. A single oscillating mode does not have a structure. The same is true for the MOPs. It may come as a surprise that the MOP-model is also somewhat deficient in this case. After all, the basic equation for $\hat{v}$ is linear and of third order. One might expect that the fit of a third-order autoregressive model yields perfect results in this case. However, from in Appendix 2 it is clear that the fit of an autoregressive model of second order to a simple damped oscillation is far from perfect if the damping is even of moderate strength. This example explains why the representation of the Rossby wave in Fig. 3 deteriorates with increasing damping rate d.

3 Nonlinear low-order system

The nonlinear system to be considered is based on a low-order model of Lorenz (1960) designed to understand the basic dynamics of the index cycle in the atmosphere. The model of Lorenz (1960) solves the inviscid barotropic vorticity equation without forcing in a double-periodic domain. An interacting triad of modes is selected where

$$\nabla^2\psi = a(t)\cos ly + f(t)\cos kx + 2g(t)\sin ly \sin kx \quad (26)$$

is the vorticity of the triad with meridional and zonal wave numbers l and k (ψ stream function). The Fourier coefficients a, f, g are the variables of the model, where the vorticity of the mean zonal flow is given by the first term on the right, that of the mean meridional flow by the second and that of a wave mode by the last one. Energy and enstrophy are conserved by the triad interaction so that an analytical solution to the basic equation is possible. The solutions turn out to be periodic.

Here, the model of Lorenz (1960) is extended by adding white noise forcing and damping so that the equations are

$$\frac{da}{dt} = -\left(\frac{1}{k^2} - \frac{1}{k^2 + l^2}\right)klfg - da + w_1, \quad (27)$$

$$\frac{df}{dt} = -\left(\frac{1}{l^2} - \frac{1}{k^2}\right)klag - df + w_2, \quad (28)$$

$$\frac{dg}{dt} = -\frac{1}{2}\left(\frac{1}{l^2} - \frac{1}{k^2}\right)klaf - dg + w_3. \quad (29)$$

Obviously, it is only the ratio $\alpha = k/l$ which matters and not the wavelengths $L_x = 2\pi/k$, $L_y = 2\pi/l$. Except for the damping there are only nonlinear terms in Eqs (27)–(29). Oscillations are entirely nonlinear if they occur at all.

Given the damping and the intensity $\langle w_i^2\rangle = \langle w^2\rangle$ of the forcing, the resulting stochastic flow is partially

characterized by its mean enstrophy

$$\langle Z\rangle = \frac{1}{2}\langle (a^2 + f^2 + 2g^2)\rangle$$

and energy

$$\langle E\rangle = \frac{1}{4}\langle (a^2/l^2 + f^2/k^2 + 2g^2/(k^2 + l^2))\rangle$$

If, on the other hand, the "adiabatic" version of Eqs (27)–(29) with $d = 0$, $\langle w^2\rangle = 0$ is integrated in time with just these values of energy and entrophy specified a spatial pattern undergoing periodic oscillations is obtained. Such oscillations may be found in the stochastic run as well, at least in modified form.

Time scales of atmospheric large-scale flow are chosen so that: $d = 10^{-6}s^{-1}$; $\langle w^2\rangle^{1/2} \sim 10^{-10}s^{-2}$. A fourth-order Runge-Kutta scheme is used to step the model equations forward in time with a time step of 1 h. A typical run is terminated after about 200 y. Both a MOP-model of second order and a POP-model are applied to the data provided by Eqs. (27)–(29). There is no data reduction so that $\mathbf{X} = (a, f, g)$.

To assess the performance of a model it is customary to project the data on POPs (e.g. von Storch and Zwiers 1999) and to estimate this way the variance that is "explained" by a POP. Alternatively, the success of an analysis can be assessed by comparing "observed" covariances to those produced by a POP or MOP model. If, for example, $\mathrm{Cov}(\tau, a', f') = \overline{a'(t)f'(t+\tau)}$ is the covariance of a and f with lag τ (a', f' deviations from mean), the POP- as well as the MOP-models provide an estimate of this covariance. It is just necessary to step forward the Yule-Walker equations for both models to obtain the covariances $(\overline{a'_n f'_{n+m}})_{M,P}$ where $mDt = \tau$ for both models with time step Dt. An obvious measure of success is

$$c_{af} = \sum_{m=2}^{L} ((\overline{a'_n f'_{n+m}})_{M,\mathrm{P}} - Cov(\tau, a, f'))^2/(\overline{a'_n f'_n})^2 \qquad (30)$$

An overall skill score is the covariance error

$$S = c_{aa} + c_{ff} + c_{gg}. \qquad (31)$$

It is clear a priori that the scores of the MOP model must be better than those of the POP model when both models are applied to the same data set. However, it is not clear a priori if the MOP approach will yield useful qualitative information in addition to that provided by the POP analysis.

The parameter $\alpha = k/l$ determines much of the dynamics of the system (Lorenz 1960). Six pairs of runs will be discussed where α varies between the pairs (Table 1). For each pair, the second run has double the forcing intensity of the first one. The period of oscillations ought to decrease with increasing forcing. Indeed, the autocorrelation of the wave variable g as displayed in Fig. 4 indicates that there are oscillations both for $\langle w^2\rangle = 1$ and $\langle w^2\rangle = 4$ but the typical period of those is shorter for the larger forcing. The stability of these autocovariances has been tested by running the model for 400 and for 600 y. The related changes were small, so that Fig. 4 provides an acceptable estimate of the autocovariances.

Table 1 Eigenvalues v_i and covariance error $S_P[10^{-2}]$ of the POP analysis for six runs with model Eqs. (27)–(29). The first entry for each of the eigenvalues is the modulus, the second is the oscillation period in days. Only one eigenvalue is given for a complex conjugate pair. Forcing amplitudes in $3 \times 10^{-10}\,\mathrm{s}^{-2}$. Time step of POP-model $Dt = 1$ day

Run	k/l	$\langle w^2\rangle^{1/2}$	v_1	v_2	v_3	S_P
1	0.95	1	0.91/-	0.82/-	0.8/-	1.8
2	0.95	2	0.91/-	0.61/-	0.5/-	1.5
3	2.0	1	0.91/-	0.53/81		0.3
4	2.0	2	0.91/-	0.22/-	0.02/-	0.5
5	0.5	1	0.90/-	0.52/107		0.3
6	0.5	2	0.90/-	0.21/-	0.02	0.5

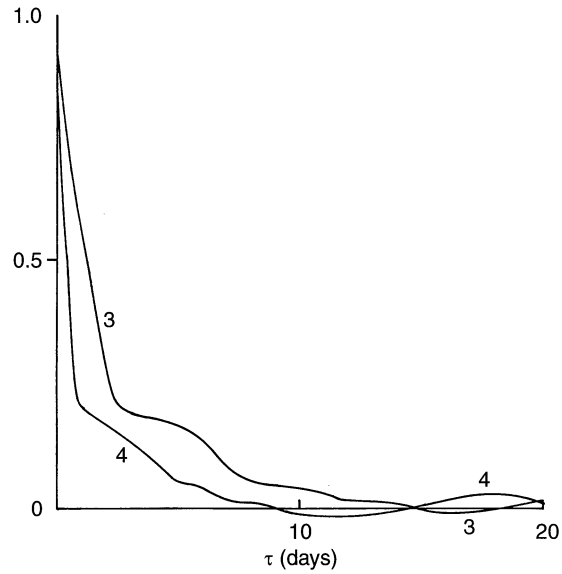

Fig. 4 Autocorrelation of variable g in runs 3, 4 (see Table 1) as a function of lag τ

The three eigenvalues v_i of the POP model and the six eigenvalues λ_i of the MOP model as well as the scores S_P, S_M are displayed in Tables 1, 2 for all six runs. The first entry is the modulus while the second entry gives the oscillation period in days. The corresponding complex conjugate eigenvalues are not given.

Except for runs 3 and 5, the POP analysis produces real eigenvalues. Moreover, the oscillation period in those runs is so long when compared to the decay rate that these oscillations are irrelevant. The eigenvalue v_1 $v = 0.91$ captures the decay through damping where $\exp(-dDt) = 0.92$. The eigenvectors for runs 1 and

5 are presented in Tables 3, 4. The first POP of run 1 describes almost exclusively red noise behaviour of g while the other two POPs link a and f. In run 5, however, the first POP describes red noise fluctuations of the zonal flow. The second POP links a and g.

The MOP-analysis gives a damped mode with $\lambda_1 \sim 0.9$ in all cases as did the POP-analysis. However, there are now oscillating modes in all runs such that the period of oscillation is short enough for the oscillations to be an important part of the flow evolution. The periods decrease with increasing forcing as expected. Of course, $S_M < S_P$ in all runs.

An intercomparison of the POPs and MOPs in Tables 3, 4 shows quite a number of similarities. For example, the patterns of red noise decay (POP 1, MOP 1) are virtually identical. However, even POP 2 and MOP 2 in Table 4 are similar. Both link f and g in an oscillating mode, while the zonal mean flow does not play a role in this pattern. However, the phase relationships differ as do, of course, the periods of oscillation. While MOP 2 oscillates with a period of 6.3 days, that of POP 2 is 107 days.

Table 2 Eigenvalues λ_i and covariance error $S_M[10^{-2}]$ of the MOP analysis for the same six runs with model Eqs (27)–(29) as in Table 1

Run	λ_1	λ_2	λ_3	λ_4	λ_5	S_M
1	0.91/-	0.65/13	0.62/16	0.005/-		0.03
2	0.91/-	0.62/6.8	0.52/8.6	5×10^{-5}/-		0.6
3	0.91/-	0.54/6.7	0.39/9.8	0.004/-		0.2
4	0.91/-	0.49/-	0.36/4.0	0.31/-	0.01/-	0.2
5	0.90/-	0.55/6.3	0.45/8.7	0.005/-		0.1
6	0.91/-	0.49/-	0.36/4.0	0.3/-	0.001/-	0.2

The first entry for each eigenvalue is the modulus, the second is the oscilation period in day. Time step of MOP-model $Dt = 1$ day. Only one eigenvalue is given for a complex conjugate pair

Table 3 POPs and MOPs of run 1. The vectors are given in the same order as the eigenvalues in Tables 1, 2. They are normalized such that a is real. First entry: real part; second entry: imaginary part

	Number	a	f	g
POP	1	0.19/0.0	− 0.007/0.0	− 0.98/0.0
	2	0.54/0.0	− 0.84/0.0	− 0.03/0.0
	3	0.87/0.0	− 0.48/0.0	− 0.05/0.0
MOP	1	0.03/0.0	− 0.02/0.0	− 0.99/0.0
	2	0.49/0.0	− 0.81/ − 0.31	− 0.06/0.003
	3	0.97/0.0	− 0.21/0.08	− 0.09/0.005
	4	0.05/0.0	− 0.01/0.0	− 0.99/0.0

Table 4 POPs and MOPs of run 5. The vectors are given in the same order as the eigenvalues in Tables 1, 2. They are normalized such that a is real

	Number	a	f	g
POP	1	0.99/0.0	0.005/0.0	− 0.02/0.0
	2	0.007/0.0	0.69/ − 0.37	− 0.61/ − 0.02
MOP	1	0.99/0.0	0.002/0.0	− 0.02/0.0
	2	0.01/0.0	0.63/0.72	0.10/0.27
	3	0.01/0.0	0.002/0.29	0.46/ − 0.84
	4	0.99/0.0	− 0.04/0.0	− 0.08/0

The mean energy $\langle E \rangle$ and enstrophy $\langle Z \rangle$ in run 5 are 147 [$m^2 s^{-2}$] and 0.28×10^{-9}[s^{-2}]. The corresponding integration of the "adiabatic" version revealed a pattern with an oscillation period of 6 days, a small oscillation amplitude for a and $|f|/|g| = 1.4$. This oscillation corresponds with MOP2 of run 5 with a first period of 6.3 days. This MOP has also a ~ 0 and $|f|/|g| = 3.4$ is larger but it must be kept in mind that too close a relationship of the adiabatic oscillation and the stochastic modes should not be expected. However, the POP-analysis fails to reproduce the correct frequency. This statement holds for all six runs. The "adiabatic" integrations yield periods of 13, 7, 6, 4, 6, 3 days in the parallel runs to runs 1–6 where energy and enstrophy coincide with the corresponding mean values obtained in the stochastic runs. As can be seen from Table 2, the agreement with the periods given by the MOP-model is excellent.

As an example, the second MOP of run 3 is presented as a pattern in Fig. 5 for the beginning of an oscillation period (bold) and two days later (dashed). Initially, there is a meridionally orientated wavy band of negative vorticity at the centre of the domain which is replaced by a positive band two days later where, however, the total amplitude is smaller because of the damping.

All in all, the MOP analysis yields better results in that oscillations are found where the POP analysis detects just red noise. Except for these oscillations, the POPs and MOPs are quite similar.

4 Conclusion

Authors von Storch et al. (1988), Xu (1992), Schnur et al. (1993) and many others have demonstrated that the POP analysis is a useful tool in geophysical data analysis. There is, however, no guarantee that the resulting POPs are always useful. In this note, data sets obtained from simple models have been exposed to the POP technique in order to see under what circumstances a POP analysis might fail. Moreover, the MOP approach has been investigated.

It is customary in POP analysis to achieve data reduction by selecting a few variables only. The example in Sect. 2 demonstrates that this may be dangerous because variables of the reduced system are governed by a differential equation which is not of first order in time. In that case the POP-analysis was seen to fail. The remedy is to extend the data basis of the POP analysis to all important variables. Alternatively, a MOP-model of correct order may be used. However, the performance of the MOP model was found to be really satisfactory only for weak damping.

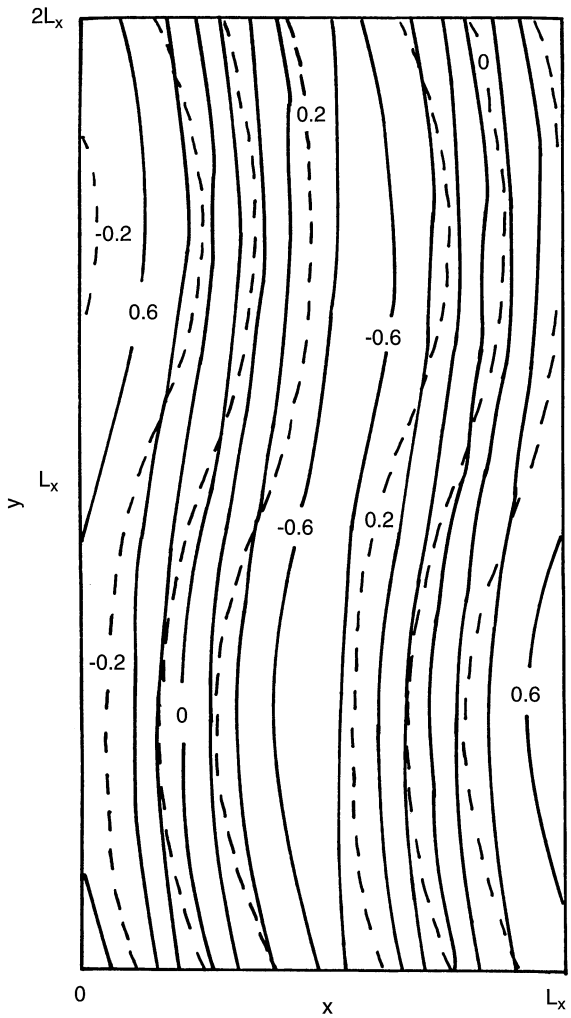

Fig. 5 Second MOP of run 3 in dimensionless units at the beginning of a damped oscillation cycle (*bold*) and two days later (*dashed*). Isopleths mark lines of constant vorticity. $\alpha = k/l = 2$

This raises the question of how to explain the success of Schnur et al.'s (1993) work. After all, Schnur et al. (1993) concentrated on the geopotential which is just one atmosphere variable out of five. Thus, the example in Sect. 2 would seem to suggest that Schnur et al. (1993) should have faced serious difficulties. However, major atmospheric dynamic systems are described rather well by the quasi-geostrophic system. This system is of first order in time and contains one variable only. Thus, a POP-analysis should provide useful answers if nonlinearity is not too strong.

On the other hand von Storch and Xu (1990) successfully applied the POP-analysis to the 30- to 60 day oscillation. These authors analyzed the 200-hPa velocity potential along the equator. The velocity potential is certainly not governed by a first-order differential equation so that there is some similarity to the example discussed in Sect. 2. Appendix 1 suggests that success is likely in this situation if the 30–60 day oscillation is clearly prominent.

For nonlinear effects, both analysis schemes capture part of the nonlinear coupling in the Lorenz (1960) model if the forcing is weak. Virtually no coupling of the modes is found for strong forcing. There are, however, oscillating MOPs while nearly all POPs are nonoscillating. These oscillations are due to nonlinearity.

Clearly, the MOP-approach is not an alternative to the POP-technique but may be used as a complementary tool. Much can be learned about the robustness of POPs and also with respect to their interpretation if the corresponding MOPs are available.

On the other hand, more data are required to construct a MOP model. Statistical significance is more difficult to achieve for the MOP matrix. This problem has been ignored in this note where either analytic expressions were available or where sufficiently long time series could be generated.

Acknowledgements I am grateful to Hans von Storch for useful comments on a draft of the work. Moreover, two anonymous referees helped considerably to clarify the presentation.

References

Box G, Jenkins G (1976) Time series analysis: forecasting and control. Helden-Dag, San Francisco; 575 pp

Bürger G (1993) Complex principal oscillation pattern analysis. J Clim 6:1972–1986

Gill A (1982) Atmosphere-ocean dynamics. Academic Press, London, pp. 434–444

Hasselmann K (1988) PIPs and POPs: the reduction of complex dynamical systems using principal interaction and oscillation patterns. J Geophys Res 93:11 015–11 021

Honerkamp J (1989) Stochastische Systeme. VCH, Weinheim, Germany, pp. 155–157

Lorenz E (1960) Maximum simplification of the dynamic equations. Tellus 12:243–254

Schnur R, Schmitz G, Grieger N, von Storch H (1993) Normal modes of the atmosphere as estimated by principal oscillation patterns and derived from quasigeostrophic theory. J Atmos Sci 50:2386–2400

von Storch H, Xu JS (1990) Principal oscillation pattern analysis of the 30- to 60-day oscillation in the tropical atmosphere. Clim Dyn 4:175–190

von Storch H, Zwiers F (1999) Statistical analysis in climate research. Cambridge University Press, Cambridge, UK, pp 349–366

von Storch H, Bruns T, Fischer-Bruns I, Hasselmann K (1988) Principal oscillation pattern analysis of the tropical 30- to 60 days oscillation in a general circulation model equatorial troposphere. J Geophys Res 93:11022–11036

von Storch H, Bürger G, Schnur R, von Storch JS (1995) Principal oscillation patterns: a review. J Clim 8: 377–400

Wilks D (1995) Statistical methods in the atmospheric sciences. International Geophysical Series 59, Academic Press, 289–357

Xu JS (1992) On the relationship between the stratospheric quasi-biennial oscillation and the tropospheric southern oscillation. J Atmos Sci 49:725–734

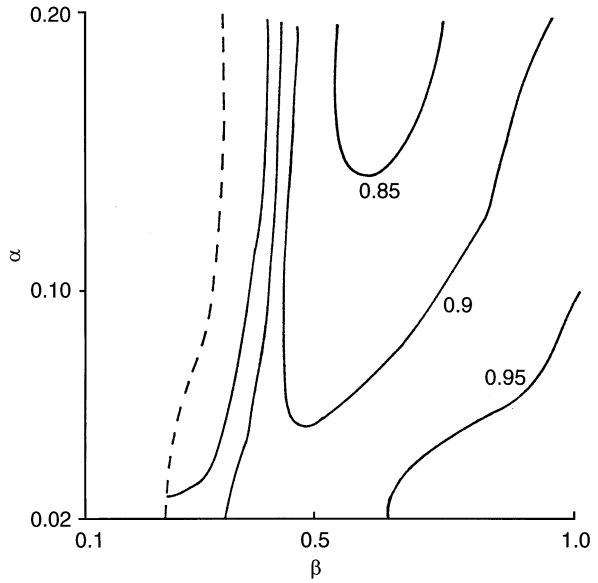

Fig. 6 Ratio of the oscillation period provided by the MOP-model (A7) to the correct period $T/2\pi$ for the range $0.02 < \alpha = dDt < 0.2$, $0.1 < \beta = Dt/T < 1$. The pattern is based on 100 data points

Appendix 1 POP-model for data with two frequencies

Assume a linear stochastic process with variables x, y where

$$\langle x^2\rangle = \langle y\rangle^2 = (A^2 + B^2)/2,$$

$$\langle x_n x_{n+1}\rangle = \langle y_n y_{n+1}\rangle = \exp(-dDt)\left(\frac{A^2}{2}\cos\omega_1 Dt + \frac{B^2}{2}\cos\omega_2 Dt\right),$$

$$\langle y_n x_{n+1}\rangle = -\langle x_n y_{n+1}\rangle = \exp(-dDt)\left(\frac{A^2}{2}\sin\omega_1 Dt + \frac{B^2}{2}\sin\omega_2 Dt\right), \quad \text{(A1)}$$

so that there are two damped oscillations, the one with amplitude A and frequency ω_1, the other one with B and ω_2. The coefficients for POP-model Eq. (22) are

$$P_{11} = P_{22} = \exp(-dDt)(A^2\cos\omega_1 Dt + B^2\cos\omega_2 Dt)/(A^2 + B^2), \quad \text{(A2)}$$

$$P_{21} = -P_{12} = \exp(-dDt)(A^2\sin\omega_1 \mathrm{Dt} + B^2\sin\omega_2 Dt)/(A^2 + \mathrm{B}^2). \quad \text{(A3)}$$

The eigenvalues of the POP-model are

$$\lambda_{1,2} = P_{11} \pm i\,P_{21}. \quad \text{(A4)}$$

If, for example, $|A| \gg |B|$, then $\lambda \sim \exp(-dDt + i\omega_1 Dt)$, so that the important mode is chosen. If, however, $A = B$, then

$$\lambda_{1,2} = \exp(-dDt)\cos((\omega_1 - \omega_2)Dt/2) \times \exp(\pm i(\omega_1 + \omega_2)Dt/2). \quad \text{(A5)}$$

In this case, the POP-model yields good results only if $\omega_1 \sim \omega_2$. The results are useless if ω_1 and ω_2 differ.

Appendix 2 Fitting of a MOP-model to a damped oscillation

Assume that a stochastic process has the autocovariance

$$c(\tau) = \cos\left(\frac{\tau}{T}\right)\exp(-d\tau) \quad \text{(A6)}$$

where d is a damping rate and $T/2\pi$ an oscillation period. An autoregressive model of second order should be of sufficient complexity to capture this process. The related equation is

$$x_{n+2} = Qx_{n+1} + Rx_n + w_n \quad \text{(A7)}$$

Standard procedures yield

$$Q = c(Dt)\,(c(2Dt) - 1)/(c(Dt)^2 - 1)$$

$$R = (c(Dt)^2 - c(2Dt))/(c(Dt)^2 - 1) \quad \text{(A8)}$$

where Dt is the time step selected for (A7). The related eigenvalue is complex with

$$|\lambda| = |R| \quad \text{(A9)}$$

Figure 6 shows the ratio of the oscillation period as obtained from the MOP-model to the correct period T as a function of $\alpha = dDt$ and $\beta = Dt/T$. It is seen that damped motion is diagnosed by the MOP-model for small β. If we accept a ratio of 0.9 as acceptable, the results of the MOP-model are satisfactory if $\beta^2 \geq 5\alpha$, at least outside the narrow range near $\beta^2 = 0.3$ where results are rather sensitive to changes of β. In other words, β must be relatively large for the MOP-model to be successful. Obviously, the Rossby wave in Sect. 2 with its large value of T meets this criterion only if d is quite small.